

Research Paper

Human Umbilical Cord MSCs as New Cell Sources for Promoting Periodontal Regeneration in Inflammatory Periodontal Defect

Fengqing Shang^{1,2,3,4*}, Shiyu Liu^{1,2*}, Leiguo Ming^{1,2*}, Rong Tian², Fang Jin^{1,4}, Yin Ding^{1,4}, Yongjie Zhang^{1,2}, Hongmei Zhang⁵, Zhihong Deng^{6*}, and Yan Jin^{1,2*}

1. State Key Laboratory of Military Stomatology & National Clinical Research Center for Oral Diseases & Shaanxi Key Laboratory of Oral Diseases, Center for Tissue Engineering, Fourth Military Medical University, Xi'an, Shaanxi 710032, China;
2. Research and Development Centre for Tissue Engineering, Fourth Military Medical University, Xi'an, Shaanxi, China;
3. Department of Stomatology, the 306th Hospital of PLA, Beijing 100101, China;
4. State Key Laboratory of Military Stomatology & National Clinical Research Center for Oral Diseases & Shaanxi Clinical Research Center for Oral Diseases, Department of Orthodontics, School of Stomatology, The Fourth Military Medical University, Xi'an, Shaanxi, 710032, China;
5. Department of Burns and Plastic surgery, Tangdu Hospital, Fourth Military University, Xi'an, Shaanxi, 710038, China;
6. Department of Otolaryngology, Xijing Hospital, Fourth Military Medical University, Xi'an, Shaanxi, 710032, China.

* Contributed equally to this work

✉ Corresponding authors: Prof. Yan Jin. State Key Laboratory of Military Stomatology & National Clinical Research Center for Oral Disease, Center for Tissue Engineering, Fourth Military Medical University, Xi'an, Shaanxi, 710032, China E-mail: yanjin@fmmu.edu.cn or Prof. Zhi-hong Deng. Department of Otolaryngology, Xijing Hospital, Fourth Military Medical University, Xi'an, Shaanxi, 710032, China. E-mail: dengzh@fmmu.edu.cn

© Ivyspring International Publisher. This is an open access article distributed under the terms of the Creative Commons Attribution (CC BY-NC) license (<https://creativecommons.org/licenses/by-nc/4.0/>). See <http://ivyspring.com/terms> for full terms and conditions.

Received: 2017.03.02; Accepted: 2017.08.18; Published: 2017.09.26

Abstract

Human periodontal ligament stem cells (hPDLSCs) transplantation represents a promising approach for periodontal regeneration; however, the cell source is limited due to the invasive procedure required for cell isolation. As human umbilical cord mesenchymal stem cells (hUCMSCs) can be harvested inexpensively and inexhaustibly, here we evaluated the regenerative potentials of hUCMSCs as compared with hPDLSCs to determine whether hUCMSCs could be used as new cell sources for periodontal regeneration.

Methods The characteristics of hUCMSCs, including multi-differentiation ability and anti-inflammatory capability, were determined by comparison with hPDLSCs. We constructed cell aggregates (CA) using hUCMSCs and hPDLSCs respectively. Then hPDLSCs-CA and hUCMSCs-CA were combined with β -tricalcium phosphate bioceramic (β -TCP) respectively and their regenerative potentials were determined in a rat inflammatory periodontal defect model.

Results hPDLSCs showed higher osteogenic differentiation potentials than hUCMSCs. Meanwhile, hUCMSCs showed higher extracellular matrix secretion and anti-inflammatory abilities than hPDLSCs. Similar to hPDLSCs, hUCMSCs were able to contribute to regeneration of both soft and hard periodontal tissues under inflammatory periodontitis condition. There were more newly formed bone and periodontal ligaments in hPDLSCs and hUCMSCs groups than in non-cell treated group. Moreover, no significant differences of regenerative promoting effects between hPDLSCs and hUCMSCs were found.

Conclusion: hUCMSCs generated similar promoting effects on periodontal regeneration compared with hPDLSCs, and can be used as new cell sources for periodontal regeneration.

Key words: Periodontal regeneration; UCMSC; Cell therapy; Inflammation microenvironment.

Introduction

Periodontitis, a common and widespread disease, can cause the irreversible destruction of the tooth supporting structure and subsequent tooth loss, if untreated [1]. Once hard (bone and cementum) and soft (periodontal ligament) connective tissues, a complex anatomical structure of the periodontium,

are lost, regeneration of the periodontium is of great clinical significance [2]. The ultimate goal of periodontal therapy is to restore the structure and function of the damaged periodontium in a spatially defined microenvironment and to control the inflammation status and progression of periodontitis.

Although conventional periodontal and/or surgical treatments usually succeed in preventing disease progression, they still cannot regenerate lost periodontal tissue or its functionality. Though various regenerative therapies, such as guided tissue regeneration (GTR) treatment [3], multiple growth factor-based treatment [4] and the application of an enamel matrix derivative [5], have been utilized, the outcomes are unsatisfactory, with poor clinical predictability [6].

With the development of progenitor cell biology and tissue engineering, cell-based therapeutics for periodontal regeneration will be more efficient and predictable to overcome the limitations of existing treatments [4, 7]. It has been postulated that stem/progenitor cells with the ability to self-renew and differentiate are the key factor in regenerative medicine, which can either be injected directly into the defect or delivered to the defect by biomaterial scaffolds or cell carriers [8-12]. A variety of cell types, including but not limited to PDLSCs, bone marrow mesenchymal stem cells, adipose-derived stem cells, alveolar periosteal cells, dental follicle cells, and dental pulp cells [13-15], have been assessed for experimental periodontal tissue regeneration in a variety of animal models [16-18]. Among these cells, PDLSCs have been shown to be capable of developing into osteoblast-like cells and cementoblast-like cells as well as producing alveolar bone, cementum and periodontal ligament-like tissues *in vivo* [19-22], showing powerful regenerative potential for periodontal tissue. In recent years, PDLSCs not only have been used in periodontal regeneration of small and big animal models including dog and swine in laboratory [23, 24], but have also been used in clinical trial [25]. Indeed, PDLSCs are the most widely used stem cells for periodontal regeneration, and are the primary candidate among dental stem cells for periodontal regenerative therapies [7]. However, since PDLSCs are isolated from extracted teeth, the clinical application of PDLSCs is highly limited by their source. Moreover, the cell properties are affected by aging and local microenvironment of the donors [26].

hUCMSCs, derived from umbilical cords, are an inexpensive and inexhaustible stem cell source. Their harvest does not require the invasive procedure of hPDLSCs and does not have the controversies of human embryonic stem cells [27]. Furthermore, hUCMSCs appeared to be primitive MSCs and exhibit high plasticity and developmental flexibility [28]. In addition, hUCMSCs have demonstrated minimal immunorejection *in vivo* and are not tumorigenic [28]. These advantages make hUCMSCs an attractive candidate for periodontal regenerative therapies. To

determine whether hUCMSCs could be used as an alternative cell source for periodontal regeneration, here we used PDLSCs as control to compare the therapeutic effects between hUCMSCs and hPDLSCs in a periodontal defect model.

In addition to the seed cell, the delivery strategy also plays an essential part in the design of cell-based periodontal therapy [4]. In this regard, cell-aggregate technology has been established as a promising strategy for cell delivery that can produce a sheet of interconnected cells. In addition, cell-aggregate technology makes it easier to detach the cells from the culture substrate, so that the natural adhesion molecules on the cell surface and cell-cell interactions remain intact [29-31]. Our previous study also demonstrated that the cell-aggregate has stronger osteogenic promotive ability and could secrete more ECM (extracellular matrix) [32]. It is an attractive periodontal regeneration approach to deliver intact cell sheets onto a diseased tooth root as this simulates the anatomical features of the periodontal ligament, whose presence is necessary for reforming the periodontal attachment between alveolar bone and root surface cementum [33].

In this study, we hypothesized that hUCMSCs could be an alternative seed cell for periodontal regeneration and had more advantages than hPDLSCs under inflammatory environments.

Materials and Methods

Cell isolation and culture

Written informed consent was approved by the Ethics Committee (Institutional Review Board for Human Subjects Research) of the School of Stomatology, Fourth Military Medical University (FMMU) and was provided by all donors or guardians for their donations and subsequent use in this research project. Following informed consent, healthy impacted premolars of three teenage patients (12-19 years) were collected, whose teeth were extracted for orthodontic purposes and were free from any recent clinical acute infection. hPDLSCs primary culture was carried out as described previously [34, 35]. Briefly, hPDLSCs were gently separated from the middle part of the root surface, cut into small pieces (1 mm³) [19, 35] and then digested with 3 mg/mL of collagenase type I and 4 mg/mL of dispase (Sigma Aldrich, St. Louis, MO, USA) for 15 min. Single-cell suspensions (2×10³ cells) were seeded and cultured in α -MEM with 10% fetal bovine serum (FBS), as described in previous reports [35]. All the hPDLSCs were used after 2-4 passages and the same passage were used for each experiment. hUCMSCs were isolated and cultured from full-term umbilical

cords of healthy babies under sterile conditions [36]. The umbilical cords were washed with phosphate-buffered saline (PBS) and outer membrane and vessels were isolated and removed. The remaining tissues were manually dissected into small blocks and plated in polystyrene tissue culture flasks with a low-glucose Dulbecco's modified Eagle's medium (L-DMEM) supplemented with 10% FBS and 1% penicillin/streptomycin (PS) (Invitrogen, Carlsbad, CA) (hUCMSCs growth medium) for 7 days. Passage 4 cells were used in this study.

Flow cytometry analysis

Cell phenotypes of early passages (P3) of cultured cells were detected by flow-cytometric analysis to measure the expression of stem cell surface markers [37]. Approximately 5×10^5 hPDLSCs & hUCMSCs adherent cells were harvested. Then, the single-cell suspension was re-suspended and incubated with antibodies for human CD29 (FITC), CD90 (PE), CD146 (PE), CD105 (PE), CD31 (PE), CD34 (PE) and CD45 (APC) (BD Bioscience, San Jose, CA, USA) at 4 °C. The samples were measured by flow cytometric analysis using a Beckman Coulter Epics XL cytometer (Beckman Coulter, Fullerton, CA, USA). The experiment was repeated at least three times.

Colony-forming unit-fibroblast (CFU-F) assays

A total of 1×10^3 single-cell suspensions of hPDLSCs or hUCMSCs (P3) were suspended in basal medium and were seeded in 10 cm diameter culture dishes (Corning, Lowell, MA, USA) for CFU-F assays. These cells were fixed with 4% paraformaldehyde and stained with 0.1% toluidine blue after 14 days of cultivation. Aggregates containing ≥ 50 cells viewed under the microscope were counted as colonies and the numbers of colonies per well was counted for contrastive analysis between the two types of cells. The experiment was repeated at least three times.

Cell proliferation assay

MTT assay was carried out to assess cell proliferation. hPDLSCs or hUCMSCs (P3) were plated into plates (Corning) at a density of 2×10^3 cells/well and cultured in basal medium. Every 24 h, the medium of 8 wells of each cell line was changed into serum-free medium and 20 μ L of 5 mg/mL MTT (3-(4,5-dimethylthiazol-2-yl)-2,5-diphenyltetrazolium bromide) solution was added to each well and incubated for 4 h. After discarding the medium, formazan salts were dissolved in 150 μ L of DMSO (dimethylsulfoxide, Sigma Aldrich), and the plate was read at 490 nm by a microplate reader (ELx800, BioTek Instruments Inc., Highland Park, USA) [38, 39]. MTT assay was carried out each day of a 7-day culture period.

In vitro osteogenic assay

The multiple differentiation capacities of hPDLSCs and hUCMSCs were examined according to previous reports [19]. Cells were cultured in osteogenic medium, i.e., basal medium supplemented with 50 mg/mL L-ascorbic-2-phosphate (MP Biomedicals, LLC, Santa Ana, CA, USA), 0.1 mM dexamethasone, and 5 mM β -glycerophosphate (Sigma Aldrich), or adipogenic medium, i.e., basal medium supplemented with 1 mM dexamethasone, 10 mM insulin, 0.5 mM 1-methyl-3-isobutylxanthine (IBMX), and 200 mM indomethacin (all from Sigma Aldrich). BCIP/NBT ALP color development kit (Beyotime, Haimen, China) was used to determine the capacity of osteogenesis differentiation of hPDLSCs and hUCMSCs according to the manufacturer's protocol, and the quantification assay was performed using Plus 5.0 software. The cells were fixed with 4% paraformaldehyde for 20 min and stained with 2% Alizarin Red S (pH 4.2) (Kermel, Tianjin, China) or 0.3% Oil Red O (Sigma). The mineralized nodules and lipid droplets were dissolved by hexadecylpyridinium chloride and isopropanol, and absorbance was quantitatively measured at 560 nm for statistical analysis, respectively.

Construction of hPDLSCs-CA and hUCMSCs-CA

A total of 3×10^5 hPDLSCs and hUCMSCs were seeded into a 6-well plate and cultured in α -MEM with 10% FBS until the cells reached 80% confluence. Then, the medium was changed to α -MEM (10% FBS) containing 50 μ g/mL vitamin C (VC), which was refreshed every 2 days. After about 10 days, white membrane structure could be observed and CA became thicker with time.

Morphological observation of cell aggregate

Harvested hPDLSCs-CA and hUCMSCs-CA were fixed with 4% paraformaldehyde overnight and examined by hematoxylin and eosin (H&E) staining. Also, scanning electron microscopy (SEM, Hitachi S-4300; EIKO Engineering, Tokyo, Japan) was used to examine the microstructure of the resultant cell sheets. Briefly, after being washed in PBS three times, cell sheets were fixed with 2.5% glutaraldehyde at 0 °C, dehydrated and dried in a critical-point dryer. The experiment was repeated at least three times.

Assessment of hPDLSCs-CA and hUCMSCs-CA niche in vitro

After 7 days of osteogenic induction, ALP staining of hPDLSCs-CA and hUCMSC-CA was performed by an ALP color development kit (Beyotime, Shanghai, China) and ALP activity was

quantified by an ALP activity detection kit (Jiancheng Bioengineering, Nanjing, China). Quantitative real-time PCR (RT-qPCR) was performed to examine the mRNA expression of ALP, Runx2 and OCN as well as extracellular matrix-related gene, fibronectin, integrin- β and collagen type I. In addition, BSP and OPN, which are strongly expressed in the native periodontium in bone and cementum, especially acellular cementum, were also detected by the RT-qPCR. Briefly, total cellular RNA was isolated from hPDLSCs-CA and hUCMSCs-CA using Trizol Reagent (Invitrogen) according to the manufacturer's standard instructions. Reverse transcription of mRNA and PCR reaction were performed as described previously [40]. Primer sequences used in this experiment are listed in Table 1. Also, expression of BSP, OPN, fibronectin, collagen type I, OCN and osteonin were detected by immunofluorescence in both cell-aggregates during the induction period. The experimental process and analysis method were as previously described [32]. The experiment was repeated at least three times.

Table 1. Specific primer sequences used for real time-polymerase chain reaction analysis.

Gene	Gene Primer sequence
ALP	Forward 5'-GGACCATCCACGTCCTCAC-3' Reverse 5'-CCTGTAGCCAGGCCATTG-3'
RUNX2	Forward 5'-CACTGGCGCTGCAACAAGA-3' Reverse 5'-CATTCCGGAGCTCAGCAGAATAA-3'
OCN	Forward 5'-CCCAGGCGCTACCTGTATCAA-3' Reverse 5'-GGTCAGCCAACCTCGTCACAGTC-3'
Fibronectin	Forward 5'-CACCCAATTCCTTGCTGGTATC-3' Reverse 5'-TATTCGGTTCCTGGTTC-3'
Integrin β 1	Forward 5'-GTGAGTGCACCCCACTACTACT-3' Reverse 5'-AAGGCTCTGCACCTGAACA CATTC-3'
COL-1	Forward 5'-CCAGAAGAACTGGTACATCAGCAA-3' Reverse 5'-CGCCATACTCGAACTGGAATC-3'
BSP	Forward 5'-GGGCAGTAGTGACTCATCCGA-3' Forward 5'-TCTTCATTGTTTTCTCTTCATTG-3'
OPN	Forward 5'-TCTGGGAGGGCTTGGTTGTC-3' Forward 5'-TTTCTTGGTCGGCGTTG-3'
TGF- β	Forward 5'-CACGTGGAGCTGTACCAGAA-3' Reverse 5'-CCGGTAGTGAACCCGTTGAT-3'
β -actin	Reverse 5'-TGGCACCCAGCACAATGAA-3' Reverse 5'-CTAAGTCATAGTCCGCCTAGAAGCA-3'

The osteogenic differentiation of hPDLSCs and hUCMSCs with lipopolysaccharide treatment

Lipopolysaccharide (LPS) treatment has been reported to impair the osteogenic potential of hPDLSCs and hUCMSCs. To compare the effects of LPS on osteogenic differentiation of hPDLSCs and hUCMSCs, LPS (10 μ g/mL, O55:B5, Sigma Aldrich) [41] was added to the osteogenic induction medium and the induction medium was changed every 3 days. At day 7, ALP staining was performed and ALP activity was quantified to compare the osteogenic differentiation of hPDLSCs and hUCMSCs. In

addition, total RNA was extracted for the analysis of TGF- β expression level by RT-qPCR.

In vivo transplantation

Both hPDLSCs-CA and hUCMSCs-CA mixed with 40 mg β -TCP particles (Shanghai, Bio-lu Biomaterials Co., Ltd) were subcutaneously implanted into the dorsal region of immunocompromised mice (4-6-week-old males; Fourth Military Medical University Animal Center, Xi'an, China) (3 animals per testing group) to further investigate the biocompatibility of hPDLSCs-CA and hUCMSCs-CA in vivo. All animal procedures complied with the committee guidelines of the Fourth Military Medical University Intramural Animal Use and Care Committee and met the NIH guidelines for the care and use of laboratory animals in this study. The nude mice were sacrificed 8 weeks post-surgery and the excised specimens were fixed in 4% neutral formaldehyde. Then, the scanning electron microscopy (SEM, Hitachi S-4300; EIKO Engineering, Tokyo, Japan) was used to observe the microstructure of resultant hPDLSCs-CA, hUCMSCs-CA, β -TCP scaffold and the excised specimens, respectively.

Animal surgical procedure and experimental design

42 adult female Sprague-Dawley rats (SD rats, 250.7 \pm 20.5 g) were obtained from the Laboratory Animal Research Centre of the Fourth Military Medical University (FMMU). All surgical procedures were performed under general anesthesia induced by intraperitoneal injection of 1% pentobarbital. Periodontitis was induced as previously described [42]. The SD rats were injected with 10 μ L of Escherichia coli LPS (1 mg/mL) at the mediolateral aspect of the first right mandibular molar, while the control group received 10 μ L of saline. This administration was repeated every other day on three separate days until the end of the 30 day experimental period. The rat periodontal defect model was modified from King et al [43, 44]. Briefly, the masseter muscle and periosteum covering the buccal surface of the mandible were separated from the bone as a flap to expose the mandible. The alveolar bone over the mandibular first molar roots and cementum covering the roots of the mandibular first molar were removed with a size 3 round-head bur (Dentsply-Sankin K. K., Tokyo, Japan). The surgical defect, which was approximately 2.5 mm \times 1.5 mm, was carried out with the assistance of 10-20x magnification by using a Leica dissecting microscope and head-mounted illumination. Both hPDLSCs-CA and hUCMSCs-CA cultured in the absence of osteogenic differentiation medium carried by the β -TCP were implanted into the

defect, with the cell aggregate side of the construct facing the denuded root surface. The mandible samples were harvested at 1 week, 4 weeks, and 8 weeks after the surgery and then were tested by micro-CT analysis at each time point. In addition, histological and morphological analyses were performed by H&E and Azan staining.

Micro CT

The Inveon micro-CT system (Siemens AG, Germany) was applied to scan the mandible samples with a source voltage of 80 kV, current of 500 mA and 14.97 mm isotropic resolution. Three-dimensional (3D) images of the defects were reconstructed from the scans by the micro-CT system software.

Histomorphometric analysis

The mandible samples harvested 8 weeks after transplantation were decalcified in 17% EDTA solution for 4 weeks and embedded in paraffin. Then, the samples were sectioned horizontally every 5 μM , and were subjected to H&E or Azan staining to locate the defect area. The formation and organization of regenerated tissues were observed using light and polarized microscopy (BX50, Olympus Optical) and were evaluated from at least 6 randomly selected fields from each specimen with Image Pro Plus 6.0 software. New bone formation was defined as the bone island observed within the defect. The percentage of new bone formation was calculated by dividing the area of the defect by the area of new bone. New cementum was defined as the mineralized tissue formed on the denuded root surface with collagen fibers inserted. The percentage of new cementum was calculated by dividing the length of the whole denuded root surface by the length of root surface with new cementum. The percentage of new periodontal ligament was calculated by dividing the length of root surface with functional new periodontal ligament attachment by the length of the whole denuded root surface.

Statistical analysis

The data were analyzed by Statistical Package for Social Science (SPSS) version 20.0. Data were assessed for normal distribution and similar variance between groups before further analysis. Significance was assessed by Student's *t* tests and analysis of variance (ANOVA). Three independent experiments were performed in all cases.

Results

Isolation and characterization of human hPDLSCs and hUCMSCs

The purified hPDLSCs and hUCMSCs were

successfully obtained from PDL tissues and full-term umbilical cords of healthy babies and propagated *in vitro* on a standard plastic surface exhibiting fibroblast-like or long fusiform morphology. Flow cytometry testing was carried out to identify the typical cell surface markers for MSCs. Based on the established controls (data not shown), both hPDLSCs and hUCMSCs were positive for the MSC markers CD29, CD90, CD146, CD105, but negative for the hematopoietic markers CD31, CD34, and CD45 (Supplementary Fig. 1). In addition, both were characterized in terms of CFU-F (Fig. 1A, B), proliferation ability (Fig. 1C), and multi-differentiation ability detected by ALP staining (Fig. 1D, F), alizarin red S staining (Fig. 1E, G) and oil red O staining (Fig. 1E, H). Both hPDLSCs and hUCMSCs displayed colony-forming ability, while the area fraction of CFU-F/200 of hPDLSCs was significantly higher than that of hUCMSCs ($P < 0.05$) (Fig. 1A, B). However, the proliferation activity of hUCMSCs was significantly higher than that of hPDLSCs after 5 days of incubation ($P < 0.05$), although they exhibited a similar proliferation rate within the first 4 days (Fig. 1C). After being cultured in osteo-inductive medium for 7 days, both hPDLSCs and hUCMSCs showed increased CFU-F ALP colonies (Fig. 1D). After being cultured in osteo-inductive medium for 21 days, mineralized extracellular matrices were observed in both hPDLSCs and hUCMSCs, as demonstrated by Alizarin Red staining (Fig. 1E). As to adipogenic differentiation, both hPDLSCs and hUCMSCs demonstrated formation of lipid droplets, as shown by oil red staining (Fig. 1E). Quantitative analysis showed that hPDLSCs had higher potential than hUCMSCs for both osteogenic and adipogenic differentiation (Fig. 1F-H).

Characterization of hPDLSCs-CA and hUCMSCs-CA

After 10 days of induction with Vc-containing medium, both hPDLSCs and hUCMSCs formed complete cell aggregate (CA) that could be detached at the edge of the dishes and showed ivory and membrane-like morphologies (Fig. 2A). H&E staining revealed that the hUCMSCs-CA contained more layers of cells and more ECM than the hPDLSCs-CA (Fig. 2B). In addition, SEM examination showed that both hPDLSCs-CA and hUCMSCs-CA established a dense film-like cell network that retained tight junctions between cells. In addition, hUCMSCs-CA showed a smoother surface compared with hPDLSCs-CA (Fig. 2C).

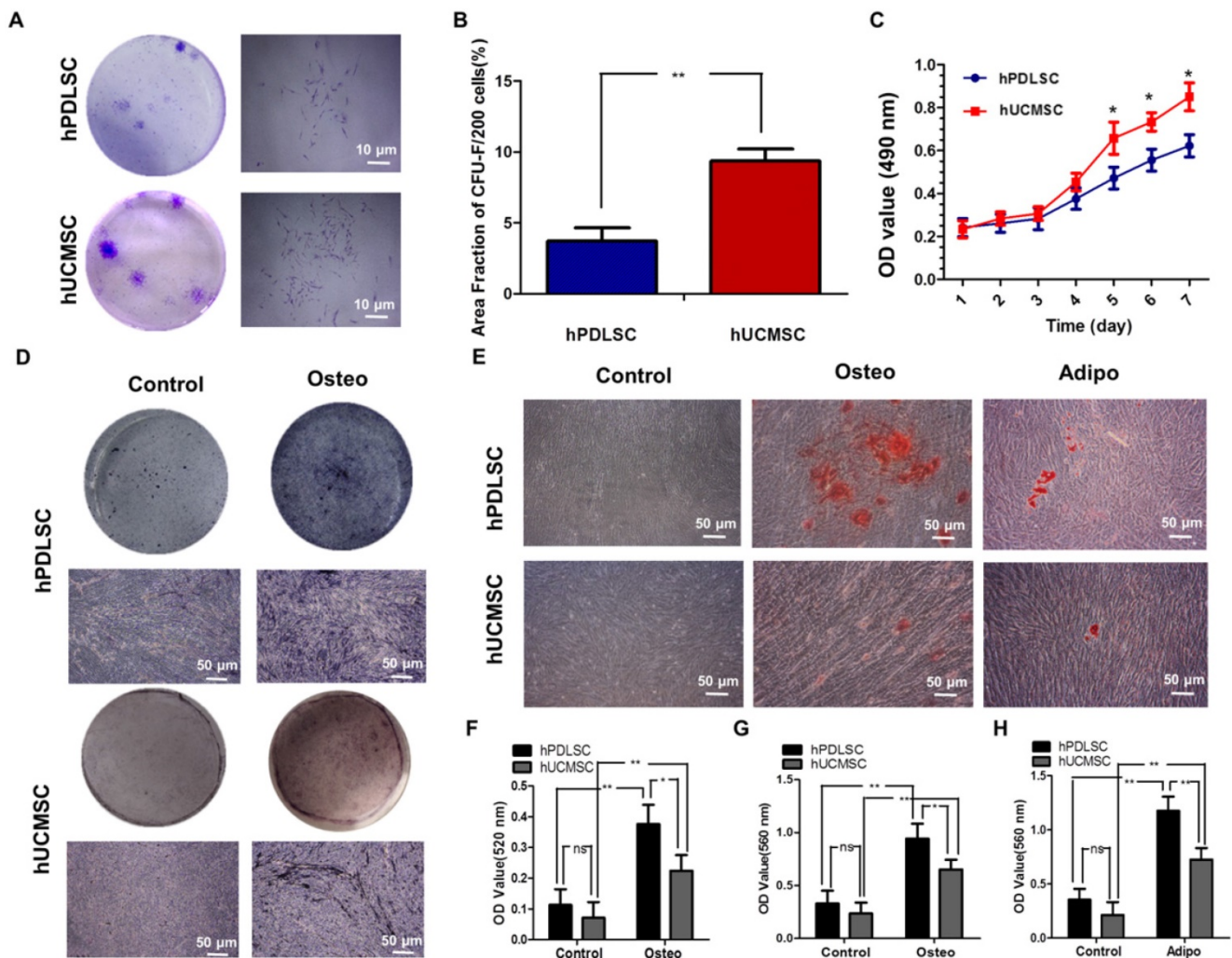


Figure 1. Isolation and characterization of human periodontal ligament stem cells (hPDLSCs) and umbilical cord mesenchymal stem cells (hUCMSCs). (A) Representative images of colony-forming unit fibroblast (CFU-F) formed by hPDLSCs and hUCMSCs at low seeding density after 14 days of culture. (B) Quantitative comparison of the total area fraction of CFU-F between hPDLSCs and hUCMSCs. (C) Growth curves of hPDLSCs and hUCMSCs determined by 3-(4, 5 dimethylthiazol-2-yl)-2, 5-diphenyltetrazolium bromide (MTT) assay. (D) Representative images of alkaline phosphatase (ALP) staining in hPDLSCs and hUCMSCs treated by osteogenic induction medium for 7 days. (E) Cultured hPDLSCs and hUCMSCs formed calcified nodules that stained positively for Alizarin Red S staining after 4 weeks of osteogenic induction, and formed Oil Red O-positive lipid droplets after 3 weeks of adipogenic induction. (F) Comparison of ALP activities between hPDLSCs and hUCMSCs treated by osteogenic induction medium for 7 days. (G) Quantitative comparison of mineralized nodule formation between hPDLSCs and hUCMSCs in normal culture medium (control) or osteogenic induction medium. (H) Quantitative comparison of lipid droplet formation between hPDLSCs and hUCMSCs in normal culture medium (control) or adipogenic induction medium. Three independent assays were performed for each cell population. $p < 0.05$ was considered statistically significant (NS, $p > 0.05$, * $p < 0.05$, ** $p < 0.01$, *** $p < 0.001$).

To assess the osteogenesis ability of CA, ALP staining was performed on hPDLSCs-CA and hUCMSCs-CA. The results indicated that the CFU-F ALP colonies (Fig. 2D) and ALP activity (Fig. 2E) of hPDLSCs-CA was significantly higher than that of hUCMSCs-CA. Additionally, the mRNA expression of ALP, Runx2 and OCN (Fig. 2F) as well as BSP and OPN (Fig. 2G) of hPDLSCs-CA were higher than that of hUCMSCs-CA. In comparison, the expression levels of ECM-related genes, including fibronectin, integrin β and collagen type I, were significantly higher in hUCMSCs-CA than in hPDLSCs-CA, as determined by RT-qPCR (Fig. 2H). Furthermore, all the results of immunofluorescence including BSP, OPN, fibronectin, integrin β , collagen type I, OCN

and osterix were in accordance with the results described above (Fig. 3A, B).

Anti-inflammatory capability of hPDLSCs and hUCMSCs

To compare the anti-inflammatory capabilities of hPDLSCs and hUCMSCs in an inflammatory microenvironment, osteogenesis differentiation and expression of anti-inflammatory factor TGF- β were explored. We found that under inflammatory condition, the osteogenesis differentiation potential of hPDLSCs is more severely impaired than that of hUCMSCs (Fig. 4A, B) ($P < 0.05$), as shown by ALP staining and ALP activity quantification. In addition, hUCMSCs showed higher expression of TGF- β than

hPDLSCs after being treated with LPS, which is a critical mediator involved in the immunosuppression response. However, there is no difference between them without LPS treatment (Fig. 4C) ($P > 0.05$).

Biocompatibility of hPDLSCs-CA+β-TCP and hUCMSCs-CA+β-TCP *in vivo*

The scaffold material, β-TCP (Fig. 4E), combined with different cell-aggregates (Fig. 4D), was subcutaneously transplanted into the dorsal region of immunocompromised mice to assess the biocompatibility. 8 weeks after transplantation, SEM examination (Fig. 4F, G) showed that both groups have good biocompatibility *in vivo*.

CA for periodontal regeneration in inflammatory periodontal defect

New bone formation

To determine the role of CA in periodontal

regeneration of inflammatory periodontal defects, we injected rats with lipopolysaccharide (LPS) and performed periodontal defect surgery to establish an inflammatory periodontal defect model. Then we used the combination of CA and β-TCP for therapy, and β-TCP alone was used as control (Supplementary Fig. 2). After LPS administration and periodontal defect surgery, no adverse post-operative sequela was observed in all animals. 3D Micro-CT reconstruction was performed to detect the newly formed bone tissues at 1 week, 4 weeks and 8 weeks post-surgery. As shown in Fig. 5, mineralized tissue covering the defect could be observed in the β-TCP, hPDLSCs-CA+β-TCP and hUCMSCs-CA+β-TCP groups, especially at 4 weeks, while in the blank group, most of the root surfaces remained exposed.

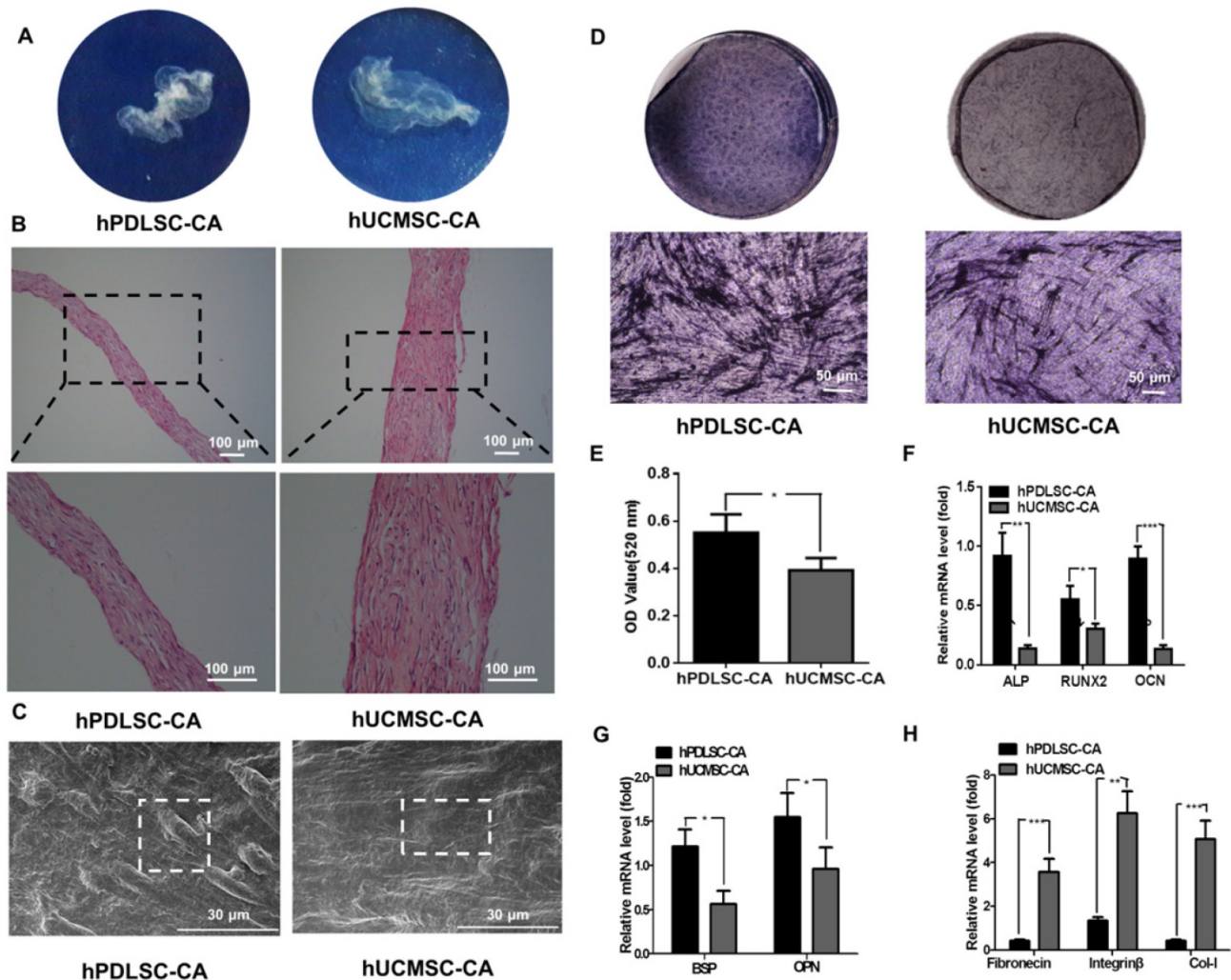


Figure 2. Morphology of hPDLSCs-CA and hUCMSCs-CA. (A) Representative macroscopic images of hPDLSCs-CA and hUCMSCs-CA plated on culture dishes. (B) Representative hematoxylin and eosin (H&E) staining images of hPDLSCs-CA and hUCMSCs-CA. (C) Representative scanning electron microscopy (SEM) images of hPDLSCs-CA and hUCMSCs-CA. (D) Representative images of ALP staining in hPDLSCs-CA and hUCMSCs-CA after osteogenic induction for 7 days. (E) Quantitative analysis of ALP activity in hPDLSCs-CA and hUCMSCs-CA. RT-qPCR analysis of the expression of classical osteogenesis associated factors (F), markers of osteoblast and cementoblast phenotypes (G) and extracellular matrix (ECM) (H) between hPDLSCs-CA and hUCMSCs-CA at the gene level.

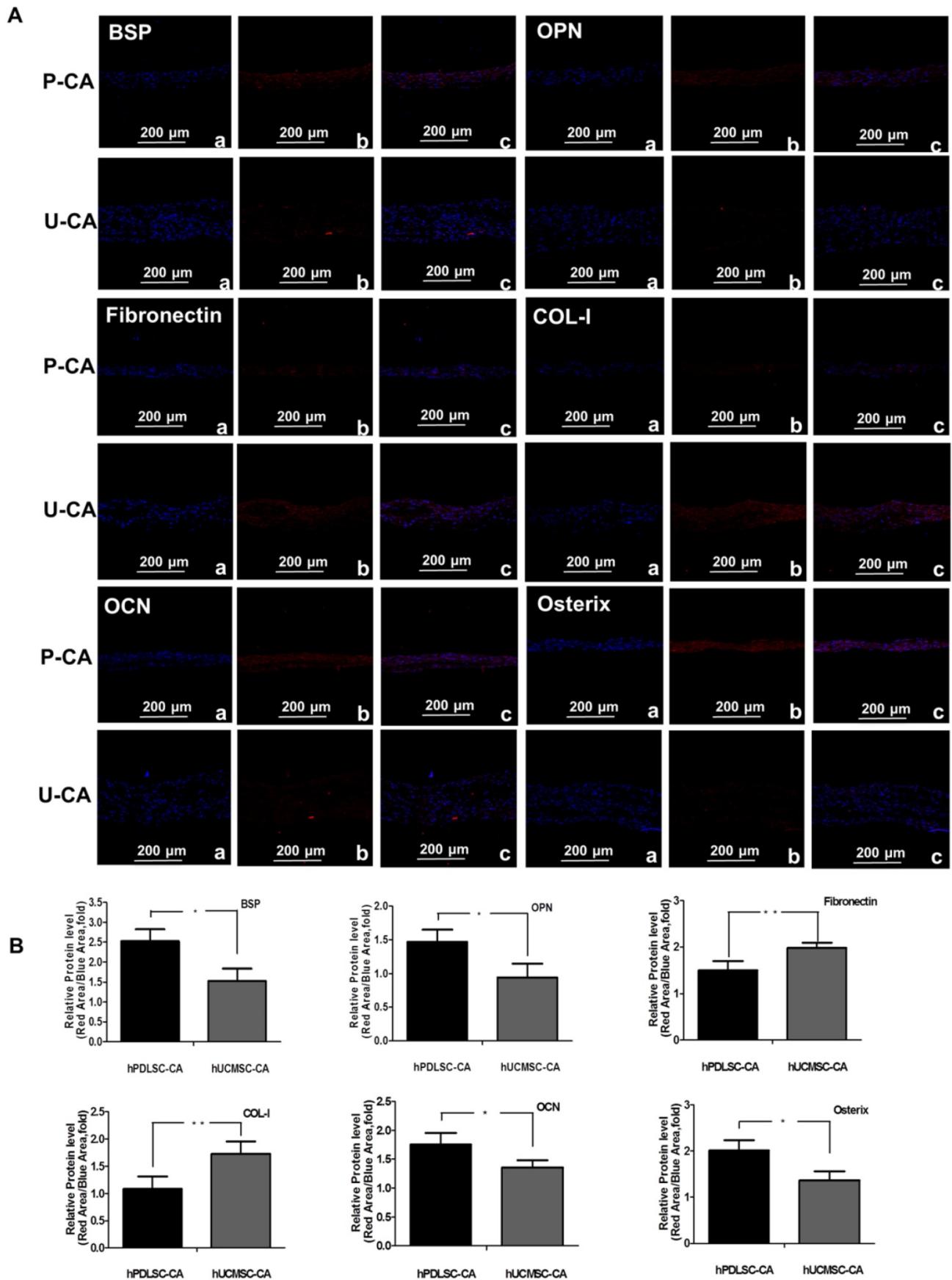


Figure 3. Characteristics of hPDLSCs-CA and hUCMSCs-CA. Immunofluorescence (A) and quantitative analysis (B) showed the expression of makers of osteoblast and cementoblast (BSP, OPN), ECM (fibronectin, Col-I) and classical osteogenesis associated factors (OCN, osterix) of hPDLSCs-CA and hUCMSCs-CA at the protein level.

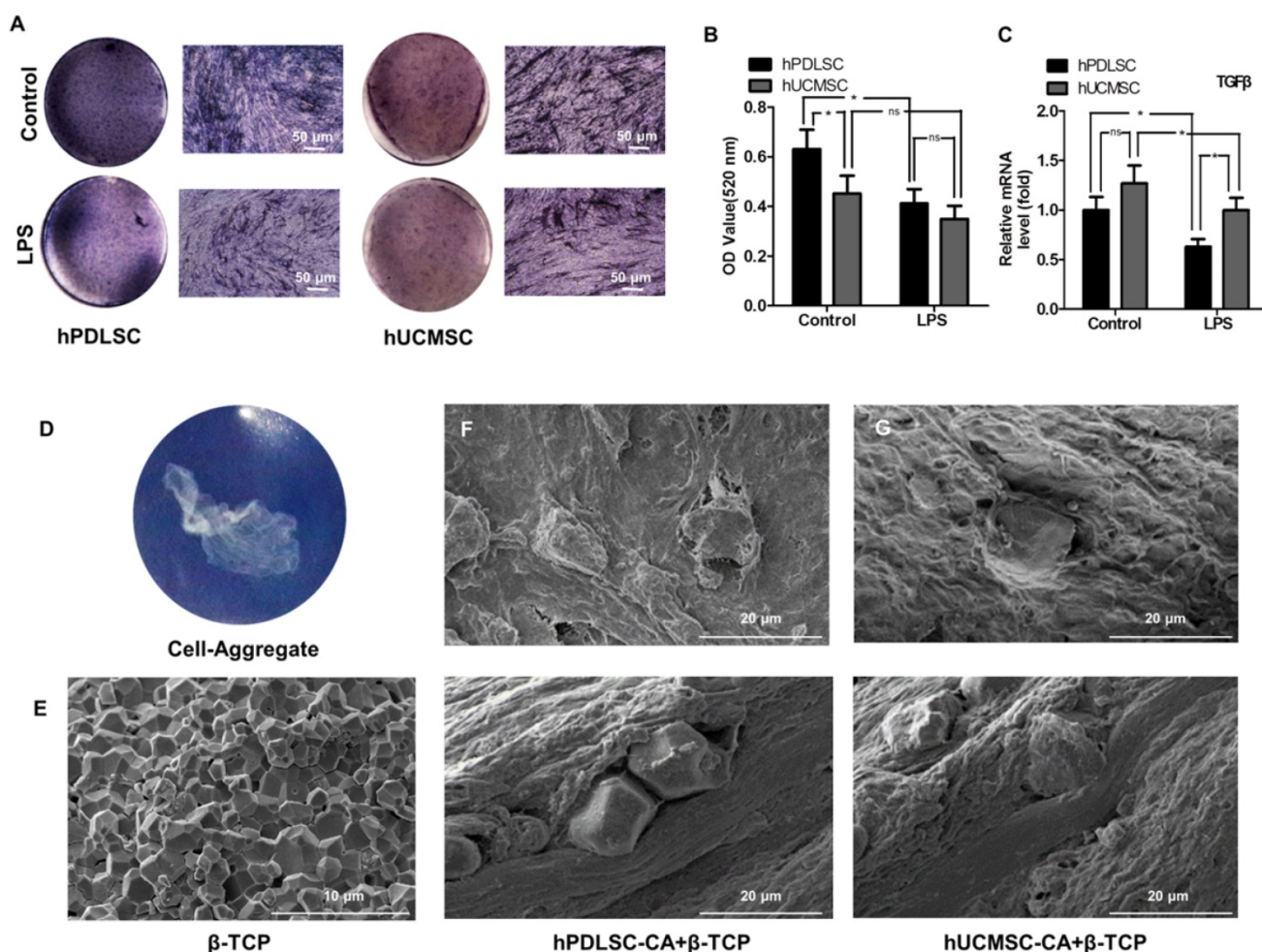


Figure 4. The anti-inflammatory capability and biocompatibility of hPDLSCs-CA and hUCMSCs-CA. hPDLSCs-CA and hUCMSCs-CA treated with or without LPS were cultured in osteogenic induction medium for 7 days, and the osteogenic ability was determined by ALP staining (A) and quantitative analyses (B). Gene expression of TGF- β in hPDLSCs-CA and hUCMSCs-CA with or without LPS treatment was measured by RT-qPCR after osteogenic induction for 7 days (C). Macroscopic image of cell aggregate (D) and scanning electron microscopy (SEM) image of β -TCP particles (E). Cell aggregates and β -TCP particles were combined and subcutaneously implanted into immunocompromised mice as indicated by SEM images of the specimens of the hPDLSCs-CA (F) and hUCMSCs-CA (G), respectively.

New bone formation also could be observed in all groups at 8 weeks after surgery, as demonstrated by histological analysis (Fig. 6A, B). The newly formed bone tissues were mainly distributed near the exposed root surfaces within the defected area (Fig. 6A). The semi-quantitative results (Fig. 6B) indicated that the β -TCP, hPDLSCs-CA+ β -TCP and hUCMSCs-CA+ β -TCP groups had a significantly higher percentage of newly formed bone than the blank group ($P < 0.05$). Although the hPDLSCs-CA+ β -TCP and hUCMSCs-CA+ β -TCP groups formed more bone tissues than the β -TCP group ($P < 0.05$), the difference between these two groups had no statistical significance ($P > 0.05$).

New cementum formation

Compared to the blank group, the hPDLSCs-CA+ β -TCP, hUCMSCs-CA+ β -TCP, and β -TCP groups generated more newly formed

cementum at 8 weeks after surgery (Fig. 6A,C) ($P < 0.05$). No significant differences were observed between the hPDLSCs-CA+ β -TCP and hUCMSCs-CA+ β -TCP groups ($P > 0.05$), both of which showed more cementum formation than the β -TCP group (Fig. 6C) ($P < 0.05$).

New periodontal ligament formation

Eight weeks post-surgery, the periodontal ligament space in all experimental groups was unmineralized. The new periodontal ligament fibers in repaired periodontium could only be observed in the hPDLSCs-CA+ β -TCP and hUCMSCs-CA+ β -TCP groups (Fig. 6E). In addition, the periodontal ligament fibers in these two groups were regularly oriented on the root surface, indicated by Azan staining (Fig. 6E). Quantitative analysis also demonstrated that the differences were not significant between these two groups (Fig. 6D, $P > 0.05$).

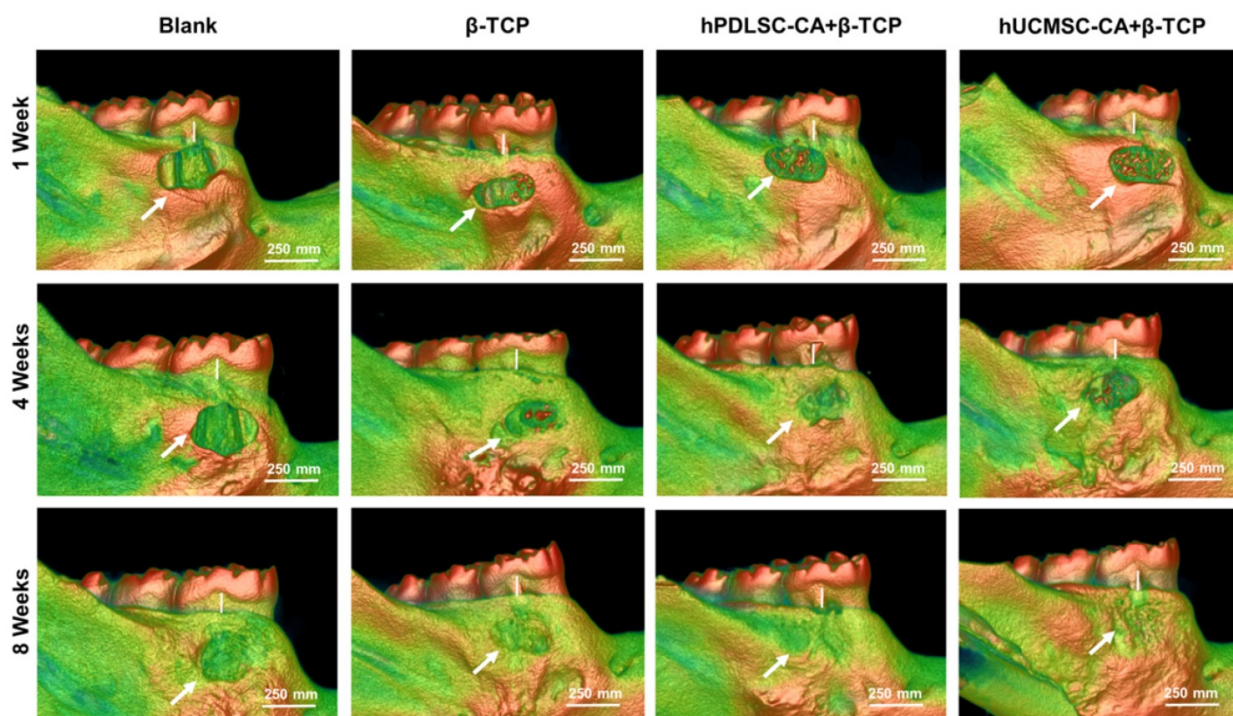


Figure 5. Representative micro CT reconstruction images of new bone formation. New bone formation (white arrow) and bone loss of alveolar bones (white bar) are shown for different groups at 1 week, 4 weeks and 8 weeks, respectively.

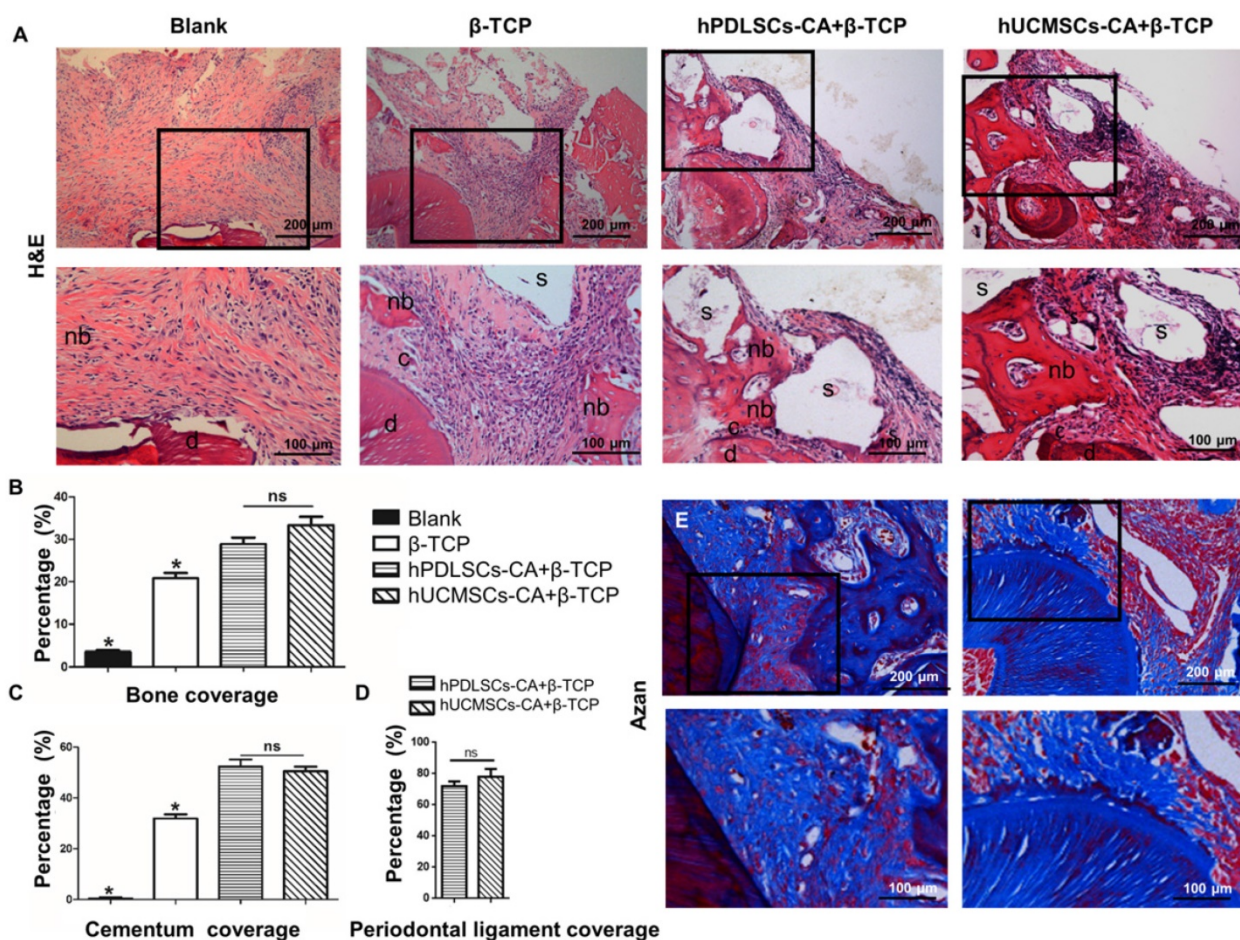


Figure 6. Histomorphometric analysis of the newly formed bone tissues, cementum and periodontal ligament fibers. Representative hematoxylin and eosin (H&E) staining (A) and Azan staining (E) indicated the formation of new bone tissues, cementum and periodontal ligament fibers at 8 weeks after surgery. (B-D) is the corresponding quantitative analysis of histomorphometry observation. c: cementum; d: dentin; s: scaffold; nb: new bone.

Discussion

Cell-based therapy represents a promising approach to achieve periodontal regeneration [4, 7]. Due to low cell activity, uneven distribution and low regeneration efficiency, a conventional technique involving single cell suspension injection showed compromised promoting effects on tissue regeneration [45]. Compared with cell sheets, cell aggregates could regenerate larger tissue defects with better morphology [46]. The aim of this study is to compare the promoting effects of hPDLSCs-CA and hUCMSCs-CA on periodontal regeneration, and determine whether hUCMSCs could be used as new cell sources for periodontal regeneration. Previous studies have already demonstrated that hPDLSCs have multiple differentiation potential [47, 48], and further proved that this kind of cell could be used for periodontal regeneration [8, 49]. The potential capability of hPDLSCs in promoting periodontal regeneration has now been demonstrated in several animal models [13, 50-54], as well as some pre-clinical trials [55, 56]. It is well established that the hPDLSCs are capable of forming new cementum on the tooth root surface and re-establishing new attachments between cementum and alveolar bone [3, 57, 58]. Thus, hPDLSCs are widely studied for periodontal regeneration.

However, one major drawback of using PDLSCs in periodontal regeneration is that the harvest of PDLSCs requires extraction of teeth. In addition, the biological behaviors of PDLSCs is closely related to age, local microenvironment and systemic conditions of the donors [26]. In addition, it is well recognized that patients who need periodontal regeneration are usually under chronic inflammatory conditions especially in the periodontal defecting area. Previous studies have already demonstrated that the osteogenic differentiation capability of hPDLSCs is significantly impaired in inflammatory microenvironment [49] with high expression of osteoclastic related factors [59]. Therefore, new cell sources for periodontal regeneration are in demand. In this regard, hUCMSCs, which are undifferentiated stem cells from infants' umbilical cords with minimal immunologic rejection, are gaining popularity in this field [60]. hUCMSCs are much younger than MSCs isolated from adult periodontium and they have high plasticity and developmental flexibility. In addition, the source of hUCMSCs is abundant and few ethical issues are associated with hUCMSCs. Our study further indicated that hUCMSCs express osteogenic differentiation markers such as ALP, Runx2 and OCN. In addition, hUCMSCs also express cementoblast phenotype related markers including

BSP and OPN [61]. Moreover, we found that hUCMSCs show extracellular matrix accumulating capability, anti-inflammatory properties and regenerative potentials under chronic inflammatory environment, indicating that hUCMSCs might be a promising cell source for periodontal defect repair.

Previous studies have already demonstrated that hUCMSCs are suitable seeding cells for regeneration of multiple kinds of tissue. In a bone fracture healing animal model, one study indicated that the osteogenic ability of UCMSCs is similar to that of BMMSCs [62]. Other researchers found that, after being cultured in neuronal induction conditioned medium for 3 days, UCMSCs expressed neuron specific proteins and could be used in nerve repair [63]. Yang et. al [64] showed that UCMSCs could even be used in regenerating damaged spinal cord. In addition, *in vivo* studies showed that UCMSCs could also significantly improve the process and prognosis of inflammatory related diseases [65], indicating that these cells have inflammation regulating ability. Our study for the first time confirmed that UCMSCs have better anti-inflammatory capability than PDLSCs, which makes them advantageous for periodontal regeneration under chronic inflammatory conditions.

One of the challenges for cell aggregate application is the difficulty in delivering and securing them onto the tooth root surface. To this end, choosing a suitable scaffold material is of critical importance in tissue engineering. Ceramics of hydroxyapatite, tricalcium phosphate (TCP) or a combination of them are widely used in studies at present. In this study, we took β -TCP as the scaffold material. This material has already been shown to exhibit good biocompatibility and osteogenic induction potential in both animal and clinical studies [50-52]. In addition, β -TCP could promote differentiation of MSCs in targeted areas [54, 55]. *In vivo* results of our study also indicated that β -TCP alone could lead to hard tissue formation in the periodontal defecting area. The combination of cell aggregates and β -TCP would further achieve periodontal attachment formation and cementum regeneration, promoting functional periodontal regeneration in animal models.

Our study focused on the periodontal regeneration using different cell aggregates under chronic inflammatory conditions. After constructing a periodontal defect animal model, LPS was injected into mandibular interdental papilla to resemble chronic inflammation condition in periodontitis [56]. It has been reported that the inflammatory conditions in this model showed high similarity to human chronic periodontitis [57, 58]. Moreover, studies have indicated that hUCMSCs could modulate the immune

response by secreting soluble factors, creating an immunosuppressive milieu [26, 49]. In the present study, hUCMSCs exhibited better immunosuppressive effect than hPDLSCs. The *in vitro* studies demonstrated that UCMSCs might display this function by secreting more TGF- β .

This study used hUCMSCs to repair periodontal tissue defects under chronic inflammation condition with the aim of finding an alternative favorable seeding cell source for periodontal regeneration. We found that, similar to hPDLSCs, hUCMSCs could promote regeneration of periodontal hard tissues under inflammatory periodontitis condition. hUCMSCs-CA could also promote the formation of new functional periodontal ligament attachments, suggesting that hUCMSCs-CA could be an alternative to PDLSCs for periodontal therapies.

Abbreviations

CA: cell aggregate; hPDLSCs: human periodontal ligament stem cells; hUCMSCs: human umbilical cord mesenchymal stem cells; LPS: lipopolysaccharide; β -TCP: β -tricalcium phosphate bioceramic.

Acknowledgements

This study was supported by the National Key Research and Development Program of China (Nos.2016YFC1101400) and Nature Science Foundation of China (81470679, 31670995, 81570976, 81500857).

Author Contributions

FQ.Sh., SY. L. and LG.M. performed the experiments and wrote the main manuscript text. R.T., F.J., and Y.D. analyzed the data. YJ. Zh. and HM. Zh. checked and revised the manuscript, ZhH. D. and Y. J. designed the project and funded this research. All authors have reviewed the manuscript before submission.

Supplementary Material

Supplementary figures.

<http://www.thno.org/v07p4370s1.pdf>

Competing Interests

The authors have declared that no competing interest exists.

References

- Pihlstrom BL, Michalowicz BS, Johnson NW. Periodontal diseases. *Lancet*. 2005; 366: 1809-20.
- Villar CC, Cochran DL. Regeneration of periodontal tissues: guided tissue regeneration. *Dental clinics of North America*. 2010; 54: 73-92.
- Nyman S, Gottlow J, Karring T, Lindhe J. The regenerative potential of the periodontal ligament. An experimental study in the monkey. *Journal of clinical periodontology*. 1982; 9: 257-65.

- Chen FM, Sun HH, Lu H, Yu Q. Stem cell-delivery therapeutics for periodontal tissue regeneration. *Biomaterials*. 2012; 33: 6320-44.
- Takeda K, Shiba H, Mizuno N, Hasegawa N, Mouri Y, Hirachi A, et al. Brain-derived neurotrophic factor enhances periodontal tissue regeneration. *Tissue engineering*. 2005; 11: 1618-29.
- Needleman IG, Worthington HV, Giedrys-Leeper E, Tucker RJ. Guided tissue regeneration for periodontal infra-bony defects. *The Cochrane database of systematic reviews*. 2006: Cd001724.
- Lin NH, Gronthos S, Bartold PM. Stem cells and future periodontal regeneration. *Periodontology* 2000. 2009; 51: 239-51.
- Yan XZ, van den Beucken JJ, Both SK, Yang PS, Jansen JA, Yang F. Biomaterial strategies for stem cell maintenance during *in vitro* expansion. *Tissue engineering Part B, Reviews*. 2014; 20: 340-54.
- Potten CS, Loeffler M. Stem cells: attributes, cycles, spirals, pitfalls and uncertainties. Lessons for and from the crypt. *Development (Cambridge, England)*. 1990; 110: 1001-20.
- Du J, Shan Z, Ma P, Wang S, Fan Z. Allogeneic bone marrow mesenchymal stem cell transplantation for periodontal regeneration. *Journal of dental research*. 2014; 93: 183-8.
- Dogan A, Ozdemir A, Kubar A, Oygur T. Healing of artificial fenestration defects by seeding of fibroblast-like cells derived from regenerated periodontal ligament in a dog: a preliminary study. *Tissue engineering*. 2003; 9: 1189-96.
- Yu N, Oortgiesen DA, Bronckers AL, Yang F, Walboomers XF, Jansen JA. Enhanced periodontal tissue regeneration by periodontal cell implantation. *Journal of clinical periodontology*. 2013; 40: 698-706.
- Tsumanuma Y, Iwata T, Washio K, Yoshida T, Yamada A, Takagi R, et al. Comparison of different tissue-derived stem cell sheets for periodontal regeneration in a canine 1-wall defect model. *Biomaterials*. 2011; 32: 5819-25.
- Dangaria SJ, Ito Y, Luan X, Diekwisch TG. Successful periodontal ligament regeneration by periodontal progenitor preseeded on natural tooth root surfaces. *Stem cells and development*. 2011; 20: 1659-68.
- Bartold PM, McCulloch CA, Narayanan AS, Pitaru S. Tissue engineering: a new paradigm for periodontal regeneration based on molecular and cell biology. *Periodontology* 2000. 2000; 24: 253-69.
- Yang Y, Rossi FM, Putnins EE. Periodontal regeneration using engineered bone marrow mesenchymal stromal cells. *Biomaterials*. 2010; 31: 8574-82.
- Tobita M, Uysal AC, Ogawa R, Hyakusoku H, Mizuno H. Periodontal tissue regeneration with adipose-derived stem cells. *Tissue engineering Part A*. 2008; 14: 945-53.
- Guo W, Chen L, Gong K, Ding B, Duan Y, Jin Y. Heterogeneous dental follicle cells and the regeneration of complex periodontal tissues. *Tissue engineering Part A*. 2012; 18: 459-70.
- Seo BM, Miura M, Gronthos S, Bartold PM, Batouli S, Brahimi J, et al. Investigation of multipotent postnatal stem cells from human periodontal ligament. *Lancet*. 2004; 364: 149-55.
- Gay IC, Chen S, MacDougall M. Isolation and characterization of multipotent human periodontal ligament stem cells. *Orthodontics & craniofacial research*. 2007; 10: 149-60.
- Shi S, Bartold PM, Miura M, Seo BM, Robey PG, Gronthos S. The efficacy of mesenchymal stem cells to regenerate and repair dental structures. *Orthodontics & craniofacial research*. 2005; 8: 191-9.
- Park JY, Jeon SH, Choung PH. Efficacy of periodontal stem cell transplantation in the treatment of advanced periodontitis. *Cell transplantation*. 2011; 20: 271-85.
- Dogan A, Ozdemir A, Kubar A, Oygur T. Assessment of periodontal healing by seeding of fibroblast-like cells derived from regenerated periodontal ligament in artificial furcation defects in a dog: a pilot study. *Tissue engineering*. 2002; 8: 273-82.
- Ding G, Liu Y, Wang W, Wei F, Liu D, Fan Z, et al. Allogeneic periodontal ligament stem cell therapy for periodontitis in swine. *Stem cells (Dayton, Ohio)*. 2010; 28: 1829-38.
- Chen FM, Gao LN, Tian BM, Zhang XY, Zhang YJ, Dong GY, et al. Treatment of periodontal intrabony defects using autologous periodontal ligament stem cells: a randomized clinical trial. *Stem cell research & therapy*. 2016; 7: 33.
- Bartold PM, Gronthos S. Standardization of Criteria Defining Periodontal Ligament Stem Cells. *Journal of dental research*. 2017; 96: 487-90.
- Zhao L, Burguera EF, Xu HH, Amin N, Ryou H, Arola DD. Fatigue and human umbilical cord stem cell seeding characteristics of calcium phosphate-chitosan-biodegradable fiber scaffolds. *Biomaterials*. 2010; 31: 840-7.
- Can A, Karahuseyinoglu S. Concise review: human umbilical cord stroma with regard to the source of fetus-derived stem cells. *Stem cells (Dayton, Ohio)*. 2007; 25: 2886-95.
- Brighton CT, Krebs AG. Oxygen tension of nonunion of fractured femurs in the rabbit. *Surgery, gynecology & obstetrics*. 1972; 135: 379-85.
- Dai J, Rabie AB. VEGF: an essential mediator of both angiogenesis and endochondral ossification. *Journal of dental research*. 2007; 86: 937-50.
- Akahane M, Nakamura A, Ohgushi H, Shigematsu H, Dohi Y, Takakura Y. Osteogenic matrix sheet-cell transplantation using osteoblastic cell sheet resulted in bone formation without scaffold at an ectopic site. *Journal of tissue engineering and regenerative medicine*. 2008; 2: 196-201.
- Shang F, Ming L, Zhou Z, Yu Y, Sun J, Ding Y, et al. The effect of licochalcone A on cell-aggregates ECM secretion and osteogenic differentiation during

- bone formation in metaphyseal defects in ovariectomized rats. *Biomaterials*. 2014; 35: 2789-97.
33. Dan H, Vaquette C, Fisher AG, Hamlet SM, Xiao Y, Huttmacher DW, et al. The influence of cellular source on periodontal regeneration using calcium phosphate coated polycaprolactone scaffold supported cell sheets. *Biomaterials*. 2014; 35: 113-22.
34. Gao LN, An Y, Lei M, Li B, Yang H, Lu H, et al. The effect of the coumarin-like derivative osthole on the osteogenic properties of human periodontal ligament and jaw bone marrow mesenchymal stem cell sheets. *Biomaterials*. 2013; 34: 9937-51.
35. Xu Q, Li B, Yuan L, Dong Z, Zhang H, Wang H, et al. Combination of platelet-rich plasma within periodontal ligament stem cell sheets enhances cell differentiation and matrix production. *Journal of tissue engineering and regenerative medicine*. 2017; 11: 627-36.
36. Wang L, Singh M, Bonewald LF, Detamore MS. Signalling strategies for osteogenic differentiation of human umbilical cord mesenchymal stromal cells for 3D bone tissue engineering. *Journal of tissue engineering and regenerative medicine*. 2009; 3: 398-404.
37. Nekanti U, Rao VB, Bahirvani AG, Jan M, Totev S, Ta M. Long-term expansion and pluripotent marker array analysis of Wharton's jelly-derived mesenchymal stem cells. *Stem cells and development*. 2010; 19: 117-30.
38. Jia TL, Wang HZ, Xie LP, Wang XY, Zhang RQ. Daidzein enhances osteoblast growth that may be mediated by increased bone morphogenetic protein (BMP) production. *Biochemical pharmacology*. 2003; 65: 709-15.
39. Chen KM, Ge BF, Ma HP, Zheng RL. The serum of rats administered flavonoid extract from *Epimedium sagittatum* but not the extract itself enhances the development of rat calvarial osteoblast-like cells in vitro. *Die Pharmazie*. 2004; 59: 61-4.
40. Liu Y, Ming L, Luo H, Liu W, Zhang Y, Liu H, et al. Integration of a calcined bovine bone and BMSC-sheet 3D scaffold and the promotion of bone regeneration in large defects. *Biomaterials*. 2013; 34: 9998-10006.
41. Li C, Li B, Dong Z, Gao L, He X, Liao L, et al. Lipopolysaccharide differentially affects the osteogenic differentiation of periodontal ligament stem cells and bone marrow mesenchymal stem cells through Toll-like receptor 4 mediated nuclear factor kappaB pathway. *Stem cell research & therapy*. 2014; 5: 67.
42. Llavanas A, Ramamurthy NS, Heikkila P, Teronen O, Salo T, Rifkin BR, et al. A combination of a chemically modified doxycycline and a bisphosphonate synergistically inhibits endotoxin-induced periodontal breakdown in rats. *Journal of periodontology*. 2001; 72: 1069-77.
43. King GN, King N, Cruchley AT, Wozney JM, Hughes FJ. Recombinant human bone morphogenetic protein-2 promotes wound healing in rat periodontal fenestration defects. *Journal of dental research*. 1997; 76: 1460-70.
44. Garcia de Aquino S, Manzolli Leite FR, Stach-Machado DR, Francisco da Silva JA, Spolidorio LC, Rossa C, Jr. Signaling pathways associated with the expression of inflammatory mediators activated during the course of two models of experimental periodontitis. *Life sciences*. 2009; 84: 745-54.
45. Ishijima M, Hirota M, Park W, Honda MJ, Tsukimura N, Isokawa K, et al. Osteogenic cell sheets reinforced with photofunctionalized micro-thin titanium. *Journal of biomaterials applications*. 2015; 29: 1372-84.
46. Na S, Zhang H, Huang F, Wang W, Ding Y, Li D, et al. Regeneration of dental pulp/dentine complex with a three-dimensional and scaffold-free stem-cell sheet-derived pellet. *Journal of tissue engineering and regenerative medicine*. 2016; 10: 261-70.
47. Nojima N, Kobayashi M, Shionome M, Takahashi N, Suda T, Hasegawa K. Fibroblastic cells derived from bovine periodontal ligaments have the phenotypes of osteoblasts. *Journal of periodontal research*. 1990; 25: 179-85.
48. Lin WL, McCulloch CA, Cho MI. Differentiation of periodontal ligament fibroblasts into osteoblasts during socket healing after tooth extraction in the rat. *The Anatomical record*. 1994; 240: 492-506.
49. Park JC, Kim JM, Jung IH, Kim JC, Choi SH, Cho KS, et al. Isolation and characterization of human periodontal ligament (PDL) stem cells (PDLSCs) from the inflamed PDL tissue: in vitro and in vivo evaluations. *Journal of clinical periodontology*. 2011; 38: 721-31.
50. Iwata T, Yamato M, Tsuchioka H, Takagi R, Mukobata S, Washio K, et al. Periodontal regeneration with multi-layered periodontal ligament-derived cell sheets in a canine model. *Biomaterials*. 2009; 30: 2716-23.
51. Flores MG, Yashiro R, Washio K, Yamato M, Okano T, Ishikawa I. Periodontal ligament cell sheet promotes periodontal regeneration in athymic rats. *Journal of clinical periodontology*. 2008; 35: 1066-72.
52. Hasegawa M, Yamato M, Kikuchi A, Okano T, Ishikawa I. Human periodontal ligament cell sheets can regenerate periodontal ligament tissue in an athymic rat model. *Tissue engineering*. 2005; 11: 469-78.
53. Nakahara T, Nakamura T, Kobayashi E, Kuremoto K, Matsuno T, Tabata Y, et al. In situ tissue engineering of periodontal tissues by seeding with periodontal ligament-derived cells. *Tissue engineering*. 2004; 10: 537-44.
54. Liu Y, Zheng Y, Ding G, Fang D, Zhang C, Bartold PM, et al. Periodontal ligament stem cell-mediated treatment for periodontitis in miniature swine. *Stem cells (Dayton, Ohio)*. 2008; 26: 1065-73.
55. Washio K, Iwata T, Mizutani M, Ando T, Yamato M, Okano T, et al. Assessment of cell sheets derived from human periodontal ligament cells: a pre-clinical study. *Cell and tissue research*. 2010; 341: 397-404.
56. Feng F, Akiyama K, Liu Y, Yamaza T, Wang TM, Chen JH, et al. Utility of PDL progenitors for in vivo tissue regeneration: a report of 3 cases. *Oral diseases*. 2010; 16: 20-8.
57. Gottlow J, Nyman S, Lindhe J, Karring T, Wennstrom J. New attachment formation in the human periodontium by guided tissue regeneration. *Case reports. Journal of clinical periodontology*. 1986; 13: 604-16.
58. Nyman S, Lindhe J, Karring T, Rylander H. New attachment following surgical treatment of human periodontal disease. *Journal of clinical periodontology*. 1982; 9: 290-6.
59. Straub RH, Cutolo M, Pacifici R. Evolutionary medicine and bone loss in chronic inflammatory diseases--A theory of inflammation-related osteopenia. *Seminars in arthritis and rheumatism*. 2015; 45: 220-8.
60. Mao F, Wu Y, Tang X, Kang J, Zhang B, Yan Y, et al. Exosomes Derived from Human Umbilical Cord Mesenchymal Stem Cells Relieve Inflammatory Bowel Disease in Mice. *BioMed research international*. 2017; 2017: 5356760.
61. Liao F, Chen Y, Li Z, Wang Y, Shi B, Gong Z, et al. A novel bioactive three-dimensional beta-tricalcium phosphate/chitosan scaffold for periodontal tissue engineering. *Journal of materials science Materials in medicine*. 2010; 21: 489-96.
62. Schneider RK, Puellen A, Kramann R, Raupach K, Bornemann J, Kneuchel R, et al. The osteogenic differentiation of adult bone marrow and perinatal umbilical mesenchymal stem cells and matrix remodelling in three-dimensional collagen scaffolds. *Biomaterials*. 2010; 31: 467-80.
63. Fu YS, Shih YT, Cheng YC, Min MY. Transformation of human umbilical mesenchymal cells into neurons in vitro. *Journal of biomedical science*. 2004; 11: 652-60.
64. Yang CC, Shih YH, Ko MH, Hsu SY, Cheng H, Fu YS. Transplantation of human umbilical mesenchymal stem cells from Wharton's jelly after complete transection of the rat spinal cord. *PloS one*. 2008; 3: e3336.
65. Mao F, Wu Y, Tang X, Wang J, Pan Z, Zhang P, et al. Human umbilical cord mesenchymal stem cells alleviate inflammatory bowel disease through the regulation of 15-LOX-1 in macrophages. *Biotechnology letters*. 2017; 39: 929-38.